

Supporting information

Structural Changes in Atomically Precise Ag₂₉ Nanoclusters upon Sequential Attachment and Detachment of Secondary Ligands

Jayoti Roy,[†] Amitabha Das,[‡] Arijit Jana,[†] Papri Chakraborty,^{§,||} Marco Neumaier,^{§,||} Horst Hahn,^{§,⊥} Biswarup Pathak,^{,‡} Manfred M. Kappes,^{*,§,||} and Thalappil Pradeep^{*,‡,#}*

[†]DST Unit of Nanoscience (DST UNS) & Thematic Unit of Excellence (TUE), Department of Chemistry, Indian Institute of Technology Madras, Chennai 600036, India

[‡]Department of Chemistry, Indian Institute of Technology Indore, Indore 453552, India

[§]Institute of Nanotechnology, Karlsruhe Institute of Technology (KIT), Kaiserstr. 12, 76131 Karlsruhe, Germany

^{||}Institute of Physical Chemistry, Karlsruhe Institute of Technology (KIT), Kaiserstr. 12, 76131 Karlsruhe, Germany

[⊥]School of Sustainable Chemical, Biological and Materials Engineering, The University of Oklahoma, Norman 73019-1004, Oklahoma, United States

[#]International Centre for Clean Water, 2nd Floor, B-Block, IIT Madras Research Park, Kanagam Road, Taramani, Chennai 600113, India

*Email: biswarup@iiti.ac.in.

*Email: manfred.kappes@kit.edu.

*Email: pradeep@iitm.ac.in. Fax: 91-44-2257-0545/0509.

Table of contents

Name	Description	Page no.
SI1	Chemicals	S3
SI2	Synthesis	S3
SI3	Concentration of stock solution	S4
Figure S1	ESI MS and structure of $[\text{Ag}_{29}]^{3-}$ NCs	S5
Figure S2	UV-vis absorbance and photoluminescence studies	S5
Figure S3	Full range ESI MS	S6
Figure S4	Structural elucidation of $[\text{Ag}_{29}]^{3-}$ NCs	S6
Figure S5	Drift time “heat-maps” of $[\text{Ag}_{29}]^{3-}$	S7
Figure S6	CID MS of L'	S7
Figure S7	Drift time and extracted MS of L'' and L''' added to $[\text{Ag}_{29}]^{3-}$	S8
Figure S8	Cis - and trans - L'	S9
Figure S9	Lowest energy DFT-optimized structures	S9
Figure S10	Comparison of bond length changes	S10
Figure S11	DFT structure of $[\text{Ag}_{29}\text{L}''\text{L}''']_1^{3-}$ and $[\text{Ag}_{29}\text{L}''\text{L}''']_1^{3-}$	S10

Experimental Section

SI1. Reagents and Materials

All the chemicals except NCs and **L'** were commercially available and used without further purification. Silver nitrate (AgNO_3 , 99.9%) was purchased from Rankem, India. Sodium borohydride (NaBH_4), 1,3-benzene dithiol (**L**), benzene-1,4-dicarbaldehyde, and ortho-aminothiophenol were purchased from Sigma-Aldrich. 1,6-Hexanedithiol was purchased directly from Sigma-Aldrich and used without further purification. Triphenylphosphine (TPP) was purchased from Spectrochem, India. All the solvents, methanol (MeOH), dichloromethane (DCM), dimethylformamide (DMF), acetonitrile (ACN), and ethanol (EtOH) were of HPLC grade ($\geq 99.9\%$) and used without further purification.

SI2. Synthesis

SI2.1 Synthesis of $[\text{Ag}_{29}](\text{TPP})_4^{3-}$ NC. $[\text{Ag}_{29}](\text{TPP})_4^{3-}$ NC was synthesized following the reported method with little modification.¹ About 20 mg of AgNO_3 was dissolved in a mixture of 5 mL MeOH and 7 mL of DCM. About 13.5 μL of **L** ligand was then added to the reaction mixture. Due to the formation of Ag-S complex upon the addition of the dithiol, the color of the solution turned yellow, immediately. The mixture was kept under stirring conditions, and shortly after this, 200 mg of PPH_3 dissolved in 1 mL of DCM was added. Soon after the addition of PPH_3 , the solution turned colorless, indicating the formation of Ag-S-P complexes. After ~15 min, 10.5 mg of NaBH_4 in 0.5 mL of ice-cold water was added. After the addition of NaBH_4 , an immediate dark-brown color was observed, which turned orange gradually, indicating the formation of the NCs. The entire reaction was carried out under dark conditions to avoid the oxidation of silver. After 4 h of continuous stirring in the dark, the reaction mixture was centrifuged, and the supernatant was discarded. The dark brown precipitate was washed repeatedly with methanol to remove all of the unreacted compounds and complexes to get purified NC. The NC were obtained as the dark brown precipitate. The precipitate was dissolved in DMF for further studies. The solution was characterized by UV-vis and ESI MS, which confirmed the formation of $[\text{Ag}_{29}]^{3-}$ NCs. However, as the NC was synthesized without the TPP ligands, they were only stable for a few hours as stated in the literature.^{1,2}

SI2.2 Synthesis of secondary ligand 2,2'-[1,4-Phenylenebis(methylidynenitrilo)] bis[benzenethiol] (L'**).** The **L'** secondary ligand was synthesized through an thermal condensation reaction following an earlier report.³ In brief, ~500 mg (3.5 mM) of benzene-1,4-dicarbaldehyde was dissolved in EtOH. ~1.125 g (~9 mM) ortho-aminothiophenol was also dissolved in MeOH-EtOH (2:1, v/v) solvent mixture. It was added dropwise to the solution at inert argon closed condition, which resulted in some yellow precipitates. As-synthesized yellow precipitates are kept for 1 day under reflux conditions. Recrystallized sample from hot DCM/hexane mixture was used for further studies. The yield of the product is 85 %. The product was soluble in various organic solvents such as DMF, DCM, MeOH, ACN.

SI2.3 Synthesis of 2-Pyreneiminethiol ligand (L''**).** The ligand was synthesized by using a reported condensation method.⁴ ~1000 mg (~4.35 mM) of pyrene aldehyde was mixed with 762 mg (~6.09 mM, 1.4 eq) of 2-aminothiophenol in an argon atmosphere. After 20 min of solid-state mixing, 20 ml MeOH and 10 ml of EtOH were added into the reaction mixture. The

solution was kept for 4 hours of reflux at 60 °C. After the reaction, the yellow-colored compound was filtered using Whatman 42 filter paper and washed several times with excess MeOH-EtOH (1:1, v/v) solvent mixture to remove the excess precursor materials and other byproducts. The formation of the product was confirmed by SCXRD and ESI MS study.

SI3. Calculation of concentration of L'/ml.

Molecular weight of L' (M): 348 gm/mL

Amount of L' taken to prepare 1 mL (V₁) stock solution (m): 3.00 mg

Amount of solvent in the reaction mixture (V₂): 8 mL

Concentration of stock solution (S₁):

1000 ml 1 (M) L' \equiv 348 gm of L'

3 mg of L': $\left(\frac{3}{0.348}\right)$ (mM) of L' in 1 mL stock

= 8.6 (mM) of L' in 1 mL stock

Amount of stock used: 0.025 mL

The final concentration (S₂) of L' in the reaction: V₁*S₁ = V₂*S₂

$$(8.6 \text{ mM} * 0.025 \text{ ml}) = (S_2 * 8 \text{ mL})$$

$$S_2 \approx 0.026 \text{ (mM)}$$

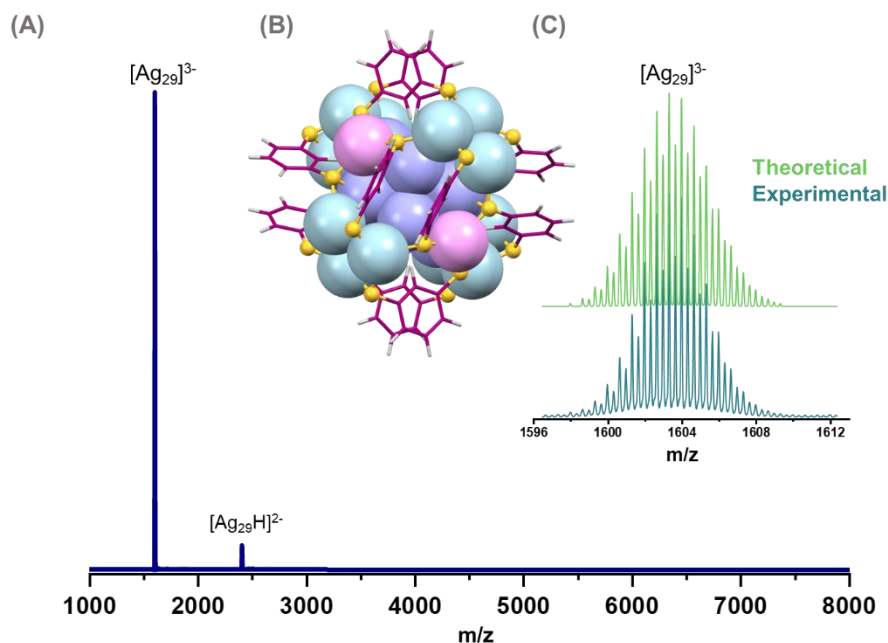


Figure S1. (A) Partial range negative ion ESI MS obtained upon dissolving as prepared $[Ag_{29}](TPP)_4^{3-}$ NC solid with counterion (see synthesis in SI2) in DMF. The MS manifests a dominant $[Ag_{29}]^{3-}$ and a weak $[Ag_{29}H]^{2-}$ multianion signal (i.e. in both cases all four TPP ligands have been detached either prior to or during ESI). Throughout the paper this is referred to simply as a $[Ag_{29}]^{3-}$ NC solution. (B) DFT optimized structure of $[Ag_{29}]^{3-}$ NCs and (C) experimental and calculated isotope patterns of the most abundant, $[Ag_{29}]^{3-}$ cluster ions.

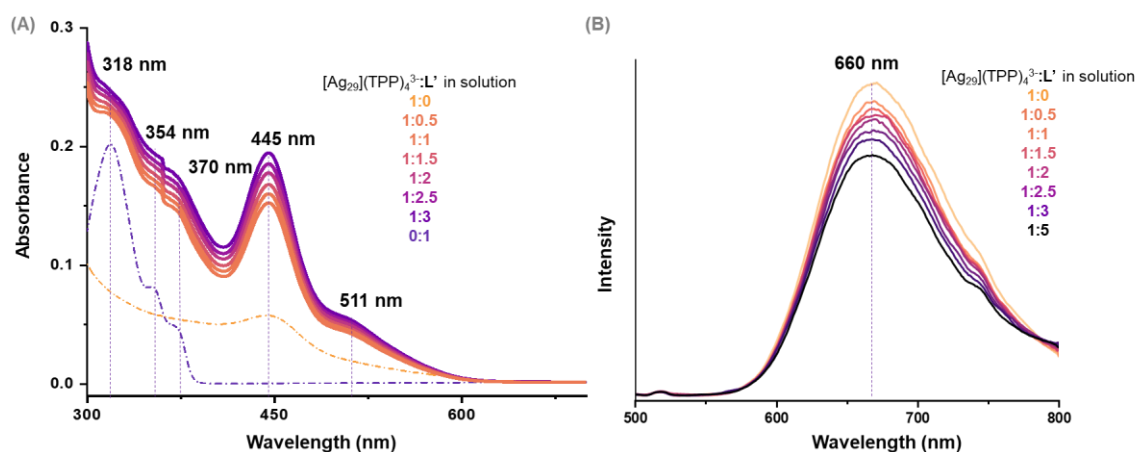


Figure S2. Sequential monitoring of (A) the UV-vis absorption spectra of $[Ag_{29}](TPP)_4^{3-}$ NCs, L' ligand, at a variable molar ratios of $[Ag_{29}](TPP)_4^{3-}:L'$ in DMF-methanol solvent. The dash-dotted spectra represent the UV-vis absorption of pure solutions of $[Ag_{29}](TPP)_4^{3-}$ NC and L' , respectively. (B) Photoluminescence spectra of $[Ag_{29}](TPP)_4^{3-}$ NCs and after adding L' to $[Ag_{29}](TPP)_4^{3-}$ NC solution at variable molar ratios upon exciting the solution at 445 nm.

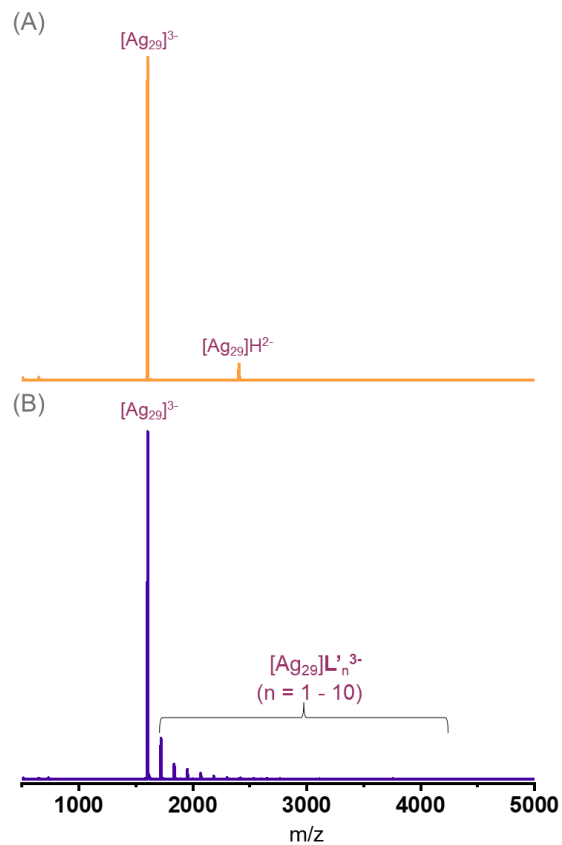


Figure S3. Full range ESI MS of m/z 500-5000 range of (A) precursor $[Ag_{29}]^{3-}$ NC, and(B) after addition of L' ligand to NC solution (in DMF solvent).

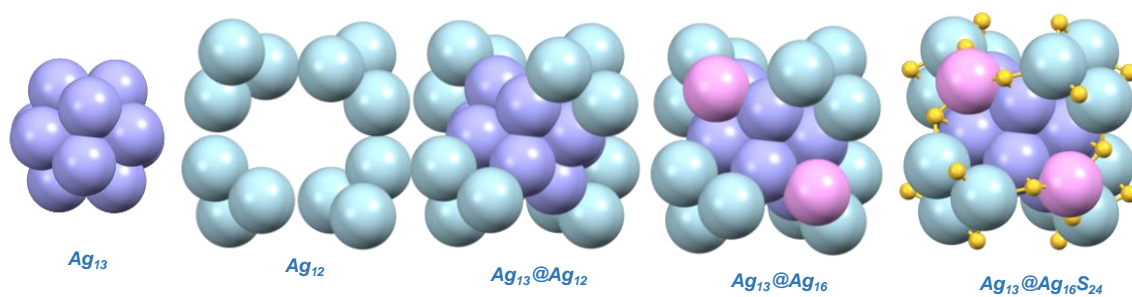


Figure S4. Schematic deconstruction of $[Ag_{29}]^{3-}$ NCs to highlight the different types of Ag atoms present in the molecule. Color code: icosahedron Ag, purple; crown Ag, pink; tetrahedral Ag, cyan blue; and sulfur (S), yellow.

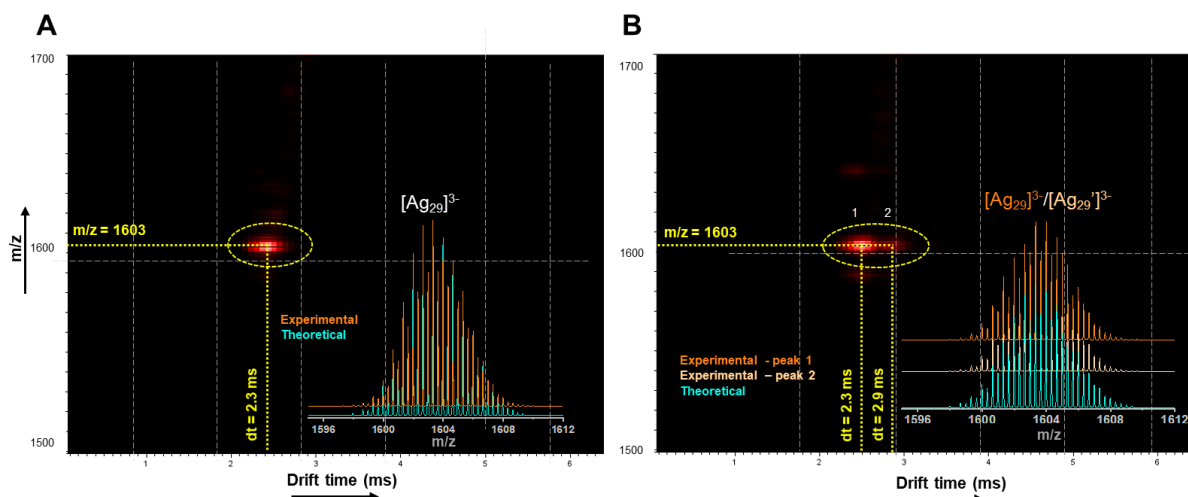


Figure S5. “Heat-map” plots recorded on the Synapt platform showing drift time (t_d) versus selected m/z recorded over the mass range of $[\text{Ag}_{29}]^{3-}$ as obtained upon electrospray of (A) a $[\text{Ag}_{29}]^{3-}$ NC solution before and (B) after adding the L' secondary ligand to it. Note that (B) shows two features at $m/z = 1603$. The extracted MS (and their simulated isotope patterns) shown in the insets confirm that the ions corresponding to both features have transited the TWIMS without (further) fragmentation. We assign them as the $[\text{Ag}_{29}]^{3-}$ parent isomer and as a larger equi- m/z isomeric $[\text{Ag}_{29}]^{3-}$ species formed by collisional detachment of L' from $[\text{Ag}_{29}(\text{L})_{12}]\text{L}'_n{}^{3-}$ upstream of the primary quadrupole mass selection.

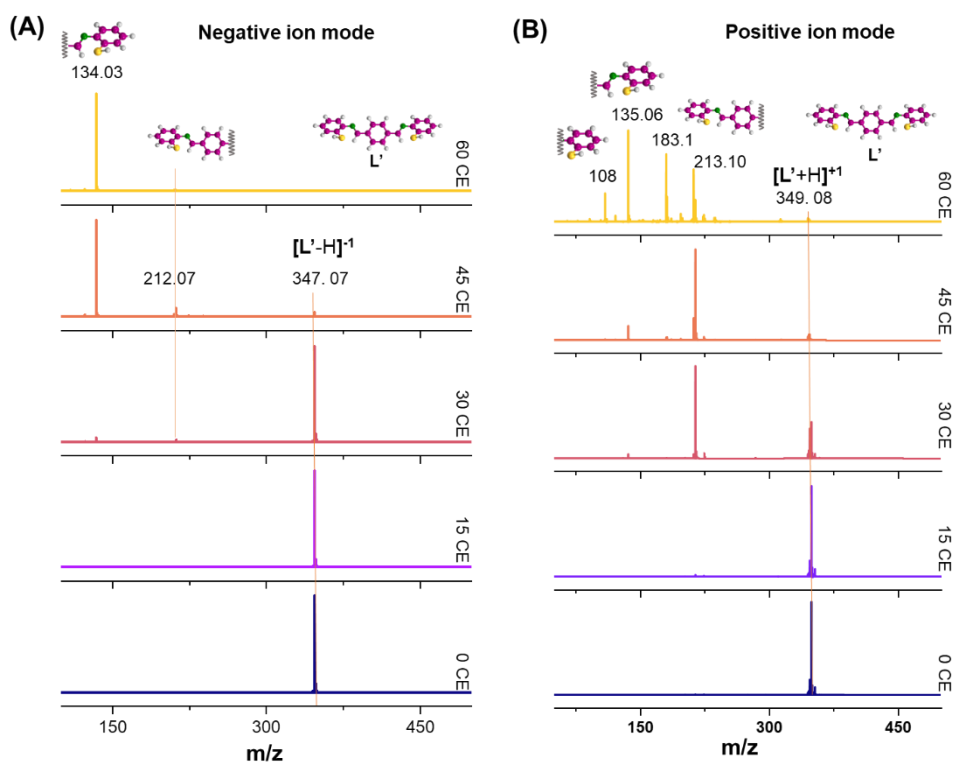


Figure S6. CID MS study to assess relative stability of $\text{L}'^{+/ -}$ ligand. (A) Probed as deprotonated $[\text{L}'-\text{H}]^-$ in negative ion mode and (B) as protonated $[\text{L}'+\text{H}]^+$ in positive ion mode as a function of collision energy (CE). Color code: S, yellow; C, dark magenta, H, light grey; N, dark green. The mass peaks generated during CID are identified with the fragment ion structures and the jagged lines also shown indicate the position of cleavage from the rest of the L' structure. Note that fragmentation of L' sets in above 15 CE and therefore does not contribute in CE 10 measurements of $[\text{Ag}_{29}(\text{L})_{12}]\text{L}'_n{}^{3-}$.

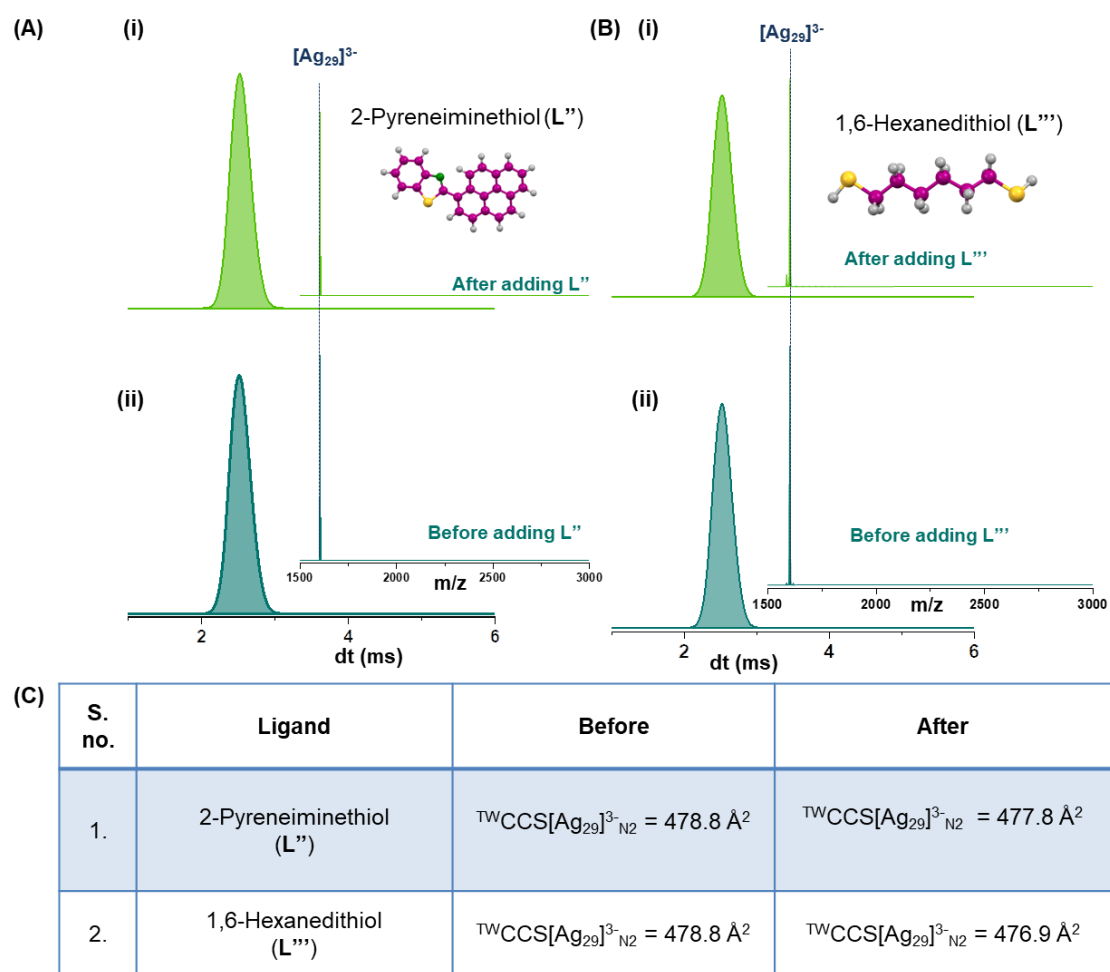


Figure S7. Drift time plots, and extracted MS of $[Ag_{29}]^{3-}$ NC solutions (i) before and (ii) after the addition of (A) L'' ligand, and (B) L''' ligands. (C) Table showing the experimental $^{TW}CCS_{N_2}$ of the $[Ag_{29}]^{3-}$ NC mass signal before and after the addition of the foreign ligands. No significant change is observed in either case. (Also, no adducts are observed in the corresponding ESI mass spectra).

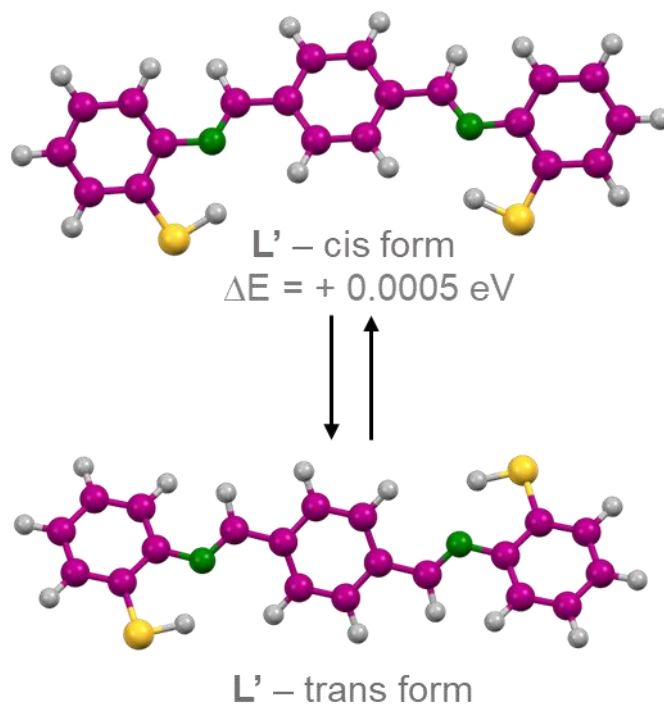


Figure S8. Optimized L' structure in cis as well as in trans form. ΔE is the relative energy difference between the cis- and the trans-L'.

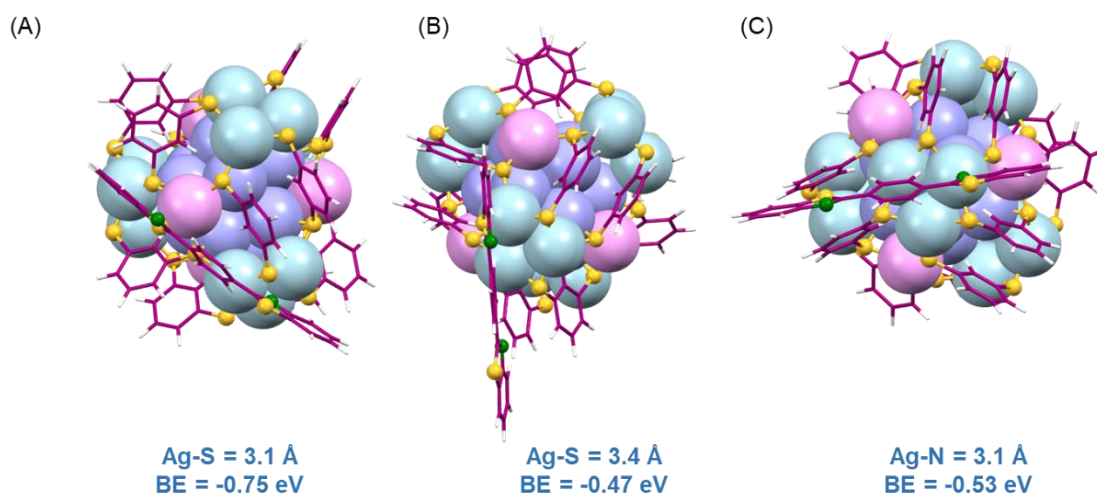


Figure S9. Lowest energy DFT-optimized structures and corresponding ligand binding energies in eV for $[\text{Ag}_{29}]\text{L}'_1^{3-}$: (A) sulfur atom of L' interacts strongly with tetrahedral Ag atom, (B) sulfur of L' interacts strongly with a crown Ag atom, (C) N of L' interacts strongly with a tetrahedral Ag atom of the NC. Color code: icosahedron Ag, purple; crown Ag, pink; tetrahedral Ag, cyan blue; and sulfur, yellow.

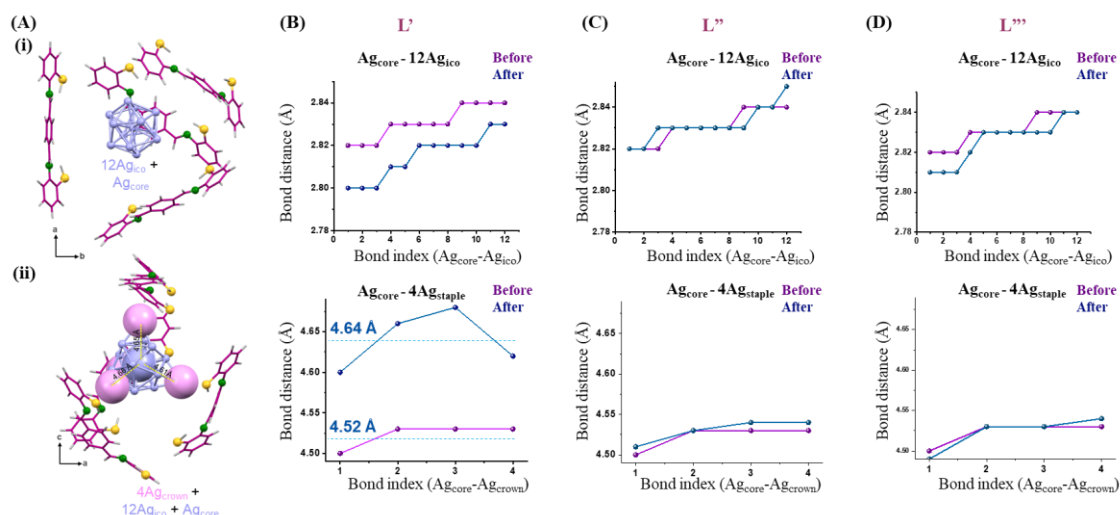


Figure S10. (A)(i) and (A)(ii) show the position of Ag_{ico}, Ag_{core}, Ag_{crown}, with respect to L' in the optimized [Ag₂₉]L'₄³⁻ structure. Tetrahedral Ag and L ligands are omitted for clarity. Comparison of bond length change between (B) [Ag₂₉]L'₄³⁻, (C) [Ag₂₉]L''₄³⁻, and (D) [Ag₂₉]L'''₄³⁻ before and after foreign ligand incorporation. Whereas L'' and L''' cause little structural change the specific interaction with L' leads to significant volume expansion.

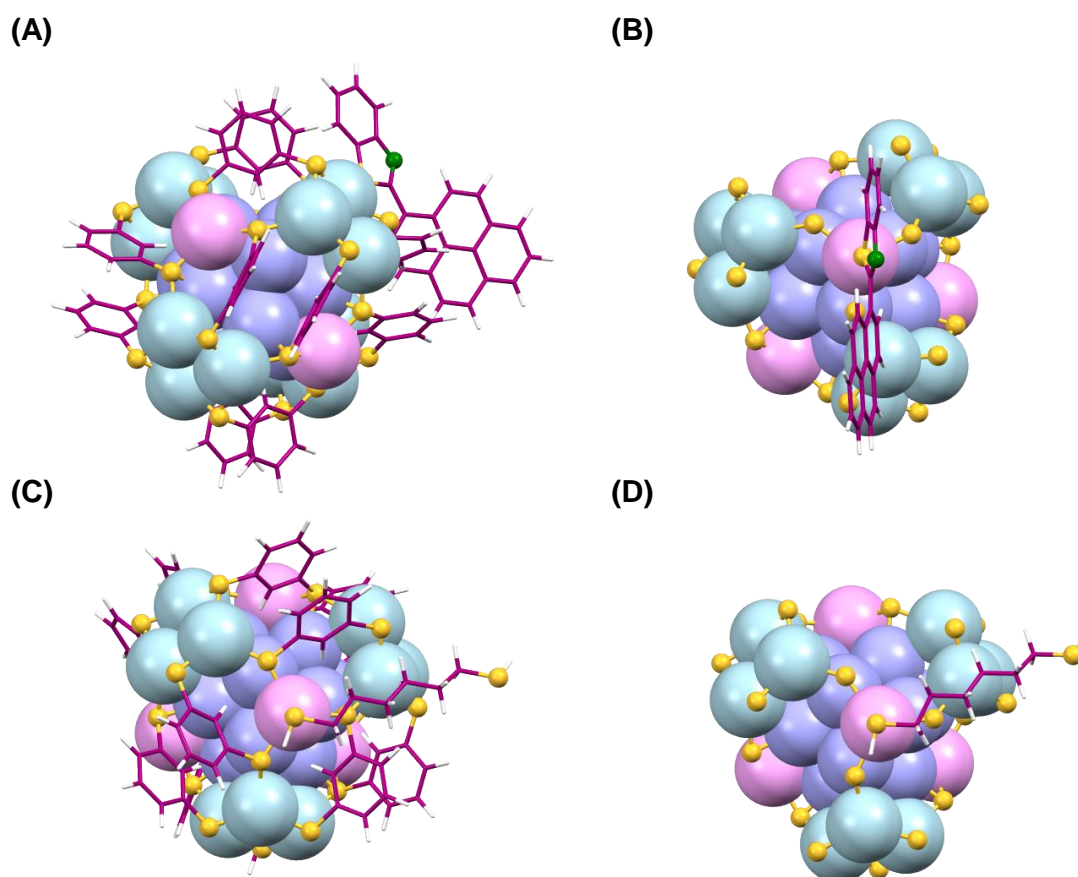


Figure S11. DFT-optimized lowest energy structures of [Ag₂₉]³⁻ NC with L'' (A) and L''' (C). For clarity, we also show the optimized structures with the phenyl ring of L removed – for L'' (B) and L''' (D), respectively. Color code: Ag, purple, pink, and cyan blue; S, yellow; C, dark magenta, H, light grey; N, dark green.

References

- (1) G. AbdulHalim, L.; S. Bootharaju, M.; Tang, Q.; Del Gobbo, S.; G. AbdulHalim, R.; Eddaoudi, M.; Jiang, D.; M. Bakr, O.; AbdulHalim, L. G.; Bootharaju, M. S.; Tang, Q.; Gobbo, S. Del; AbdulHalim, R. G.; Eddaoudi, M.; Jiang, D.; Bakr, O. M. Ag₂₉(BDT)₁₂(TPP)₄: A Tetravalent Nanocluster. *J. Am. Chem. Soc.* **2015**, *137* (37), 11970–11975. <https://doi.org/10.1021/JACS.5B04547>.
- (2) Nag, A.; Chakraborty, P.; Paramasivam, G.; Bodiuzzaman, M.; Natarajan, G.; Pradeep, T. Isomerism in Supramolecular Adducts of Atomically Precise Nanoparticles. *J. Am. Chem. Soc.* **2018**, *140* (42), 13590–13593. <https://doi.org/10.1021/jacs.8b08767>.
- (3) Wang, X.; Li, G.; Li, X.; Zhu, D.; Shen, R. One-Pot Three-Component Reaction of p-Quinone Monoacetals, L-Proline and Naphthols to Afford N-Aryl-2-Arylpyrrolidines. *Org. Chem. Front.* **2021**, *8* (2), 297–303. <https://doi.org/10.1039/D0QO01294G>.
- (4) Jana, A.; Chakraborty, P.; Dar, W. A.; Chandra, S.; Khatun, E.; Kannan, M. P.; Ras, R. H. A.; Pradeep, T. Dual Emitting Ag₃₅ Nanocluster Protected by 2-Pyrene Imine Thiol. *Chem. comm.* **2020**, *56* (83), 12550–12553. <https://doi.org/10.1039/D0CC03983G>.